arXiv:1407.0850v3 [astro-ph.HE] 20 Dec 2014

Magnetic fields and cosmic ray anisotropies at TeV energies

Eduardo Battaner, Joaquín Castellano, Manuel Masip

Departamento de Física Teórica y del Cosmos
Universidad de Granada, E-18071 Granada, Spain

battaner@ugr.es, jcastell@correo.ugr.es, masip@ugr.es

Abstract

Several cosmic-ray observatories have provided a high accuracy map of the sky at TeV–PeV energies. The data reveals an $O(0.1\%)$ deficit from north galactic directions that peaks at 10 TeV and then evolves with the energy, together with other anisotropies at smaller angular scales. Using Boltzmann equation we derive expressions for the cosmic-ray flux that fit these features. The anisotropies depend on the local interstellar magnetic field $\vec{B}_{IS}$, on the average galactic field $\vec{B}_R$ in our vicinity, and on correlations between fluctuating quantities. We show that the initial dipole anisotropy along $\vec{B}_{IS}$ can be modulated by changes in the global cosmic ray flow, and that a variation in the dipole direction would imply a given radius of coherence for the local $\vec{B}_{IS}$. We also show that small and medium-scale anisotropies may appear when the full-sky anisotropy finds a field configuration acting as a magnetic lens.

1 Introduction

We observe charged cosmic rays (protons and atomic nuclei) with energies of up to 10^{11} GeV. Although in their way to the Earth these particles lose directionality, they carry important information about their sources and about the environment where they have propagated. For example, the observation that Boron is more frequent in cosmic rays (CRs) than in the solar system suggests that it is produced when heavier nuclei *break* in their way to the Earth, implying that they cross an average depth of 10 g/cm^2 of interstellar (IS) baryonic matter in their trajectory from the dominant sources [1].

At TeV energies magnetic fields trap charged CRs in the IS medium, and their transport is usually modeled by a diffusion equation [2]. One expects that the CR gas propagates along the parallel and the perpendicular directions to the background field $\vec{B}$ with different diffusion coefficients, scattering with the magnetic turbulences $\delta\vec{B}$ in the plasma. In particular, if we define the Larmor radius

$$r_L = \frac{E}{QBc} = \left(\frac{E}{1\ \mathrm{TeV}}\right)\left(\frac{1\ \mu\mathrm{G}}{B}\right)\left(\frac{e}{Q}\right)\ 1.1\times 10^{-3}\ \mathrm{pc} \tag{1}$$

a CR will predominantly be diffused by magnetic irregularities of wave number $k \approx 1/r_L$. In a first approximation, one may picture its trajectory as an helix along $\vec{B}$ of radius $r_L\sqrt{1-\mu^2}$ and velocity

$$v_\parallel = c\mu\,, \quad v_\perp = c\sqrt{1-\mu^2}\,, \tag{2}$$

with random changes in $v_\parallel$ after a parallel mean free path $\lambda_\parallel$. Such change will also imply a variation in the field line trapping the CR, *i.e.*, $\lambda_\perp \approx r_L$.

A diffusion equation admits a multipole expansion [3] with isotropy at order zero and a dipole along the gradient direction at first order. However, this information is deduced *a posteriori*, as in a diffusion equation the momenta of the gas particles have been averaged. Boltzmann equation, instead, gives the evolution in phase space of the statistical distribution function $f(\vec{r},\vec{p};t)$ (density of particles at $\vec{r}$ with momentum $\vec{p}$), providing a microscopic description of the fluid [4, 5]. It is easy to see that when we measure the CR differential flux $F(\vec{u},E;t)$ (number of particles crossing the unit area from a given direction $\vec{u}$ per unit solid angle, energy and time) we can directly *read* the distribution function:

$$f(\vec{r}_{Earth}, -\frac{E}{c}\vec{u};t) = \frac{c^2}{E^2}\,F(\vec{u},E;t)\,, \tag{3}$$

where we have taken the relativistic limit with $E = cp$. Therefore, it is interesting to explore how the appearance of anisotropies may be explained with Boltzmann equation, specially in an environment with regular magnetic fields at different scales (see below).

In this article we will attempt a description of several large and medium scale anisotropies observed in the CR flux by several experiments. The combined results from TIBET [6], MILAGRO [7], ARGO-YBF [8], SuperKamiokande [9], ANTARES [10], IceCube [11, 12] and HAWC [13] provide a picture of the whole sky at different energies. The data reveals that the almost perfect isotropy is broken by a $O(10^{-3})$ dipole-like feature that appears at 1 TeV and evolves with the energy, together with other irregularities at lower angular scales [14, 15].

It seems clear that the direction of the local IS magnetic field $\vec{B}_{IS}$ should be a key ingredient in the explanation of these anisotropies [16]. Voyager data [17] on the heliospheric boundary provides an estimate for the direction of $\vec{B}_{IS}$:

$$\ell_B = 217^o \pm 14^o\,; \quad b_B = -49^o \pm 8^o \tag{4}$$

(in galactic coordinates), whereas IS atom measurements with IBEX [18] imply

$$\ell_B = 210.5^o \pm 2.6^o\,; \quad b_B = -57.1^o \pm 1.0^o\,. \tag{5}$$

Although the region of coherence of such field is unknown (it could vary from 0.01 to 10 pc), it is much larger than the gyroradius of a TeV cosmic ray (in Eq. (1)). At even larger distances (above 10 pc) the average magnetic field $\vec{B}_R$ can be measured using a variety of methods [19, 20, 21, 22, 23]: polarized thermal dust emission from clouds, Zeeman splitting of lines or Faraday rotation of polarized galactic and extragalactic sources, among others. The data seems to reveal a $B_R \approx 3\ \mu$G field pointing clockwise ($\ell_B \approx 90^o$) in the galactic plane ($b_B \approx 0^o$) [21]. We will also study the role that this global magnetic field plays in the explanation of the CR anisotropy.

In Section 2 we start by discussing the anisotropy that would be expected for a single CR source and an isotropic propagation. We then use Boltzmann equation to analyse how the anisotropy is deformed by the presence of a magnetic field $\vec{B}_{IS}$. We will assume that the dominant CR sources are beyond the region of coherence of $\vec{B}_{IS}$ and that their effect is captured by boundary conditions. In Section 3 we review the trajectory of CRs in the absence of turbulences. In particular, we study the *image* of a point-like source and show that there are many trajectories connecting the source with a given observer. Such study will be necessary to understand the appearence of small and medium-scale anisotropies. In sections 4 and 5, respectively, we analize the data and sumarize our results.

2 Large-scale anisotropies

Let us first consider the simplest flux: a CR gas from a pointlike source S propagating through a turbulent but homogeneous and isotropic medium. Such medium would correspond to the absence of regular magnetic field $\vec{B}_{IS}$ (or to the presence of a field weaker than the fluctuations $\delta\vec{B}$ of wave number $k \approx 1/r_L$), and it implies the same diffusion coefficient κ in all directions. The trajectories will define in this case a three-dimensional random walk of step $\lambda = 3\kappa/c$. The mean displacement D from the source that a particle reaches after a (large) time t is then [2]

$$D = \sqrt{2\kappa t}\,. \tag{6}$$

The expression above implies that the radial velocity of the gas (we call it the *CR flow*, since an observer moving at that velocity would observe an isotropic flux) will decrease like $1/\sqrt{t}$ with the distance D from S:

$$v_{\rm gas} \approx \sqrt{\frac{2\kappa}{t + 2\kappa/c^2}} = c\left(\frac{c^2 D^2}{4\kappa^2} + 1\right)^{-1/2}\,. \tag{7}$$

The relative difference between the CR flux going away or towards the source (the forward-backward asymmetry A^{FB}) can then be estimated as the ratio

$$A^{FB} \approx \frac{v_{\rm gas}}{c} \approx \frac{2\kappa}{cD}\,. \tag{8}$$

This means that the point-like source will introduce an anisotropy in the CR flux proportional to $1/D$ and to λ. Basically, it is a dipole anisotropy with the excess pointing towards S:

$$F(\vec{u}) = F_0\,(1 + \vec{u}\cdot\vec{d})\,, \tag{9}$$

where

$$\vec{d} = \frac{A^{FB}}{2\pi}\,\vec{u}_S\,. \tag{10}$$

When there are several sources S_i, it is straightforward to show that the addition of the corresponding dipole anisotropies $\vec{d}_i$ gives *another* dipole $\vec{d}$ [25]:

$$\vec{d} = \frac{\sum_i F_0^{(i)}\,\vec{d}_i}{\sum_j F_0^{(j)}}\,. \tag{11}$$

In summary, for an isotropic CR propagation we may expect a dipole anisotropy pointing towards the average CR source [27], with its intensity inversely proportional to the distance to these sources and proportional to the mean free path between collisions. Notice, however,

that the presence of a regular magnetic field $\vec{B}_{IS}$ will introduce an asymmetry between the parallel and the perpendicular diffusion coefficients ($\kappa_\parallel$ and $\kappa_\perp$) that will change this result.

To find out how, let us assume a local $\vec{B}_{IS}$ coherent over distances $R_{IS} \gg r_L, \lambda_\parallel$, with $\lambda_\parallel = 3\kappa_\parallel/c$. We will treat the CRs (protons of energy between 1 and 1000 TeV) as a fluid that only interacts with the magnetic fields. To obtain the average CR anisotropy in our vicinity we will separate the magnetic field and the distribution function into a regular plus a turbulent component,

$$\begin{array}{rcl} f & \rightarrow & \bar{f} + \delta f \ , \\ \vec{B} & \rightarrow & \vec{B}_{IS} + \delta\vec{B} \ . \end{array} \tag{12}$$

with

$$\langle\, \delta\vec{B} \,\rangle = \langle\, \delta f \,\rangle = 0 \ , \tag{13}$$

and we will *average* Boltzmann equation over nearby points. Given the relatively small distance and time scales, we will take stationary and homogeneous magnetic field $\vec{B}_{IS}$ and distribution function $\bar{f}$. We are then assuming that the CR sources are far enough so that the spatial gradient $\nabla_r \bar{f}$ is negligible (*i.e.*, smaller than $\delta f/R_{IS}$), that the changes in f occur on time scales much larger than the period of data taking (the movement of the Earth around the Sun introduces irregularities of order 10^{-4}, *i.e.*, a 10% correction to the large scale anisotropy under consideration), and we ignore energy loss or collisions with IS matter. For a fixed CR energy, $\bar{f}$ must satisfy Boltzmann equation:

$$\vec{F} \cdot \nabla_u \, \bar{f}(\vec{u}) = e \, (\vec{u} \times \vec{B}) \cdot \nabla_u \, \bar{f}(\vec{u}) = 0 \ , \tag{14}$$

where $\vec{u} = \vec{p}/p$ and $\vec{p}$ is the momentum of the CR. The equation above can also be written

$$\vec{u} \cdot \left(\vec{B} \times \nabla_u \, \bar{f} \right) = 0 \ , \tag{15}$$

which admits the generic solution

$$\bar{f}(\vec{u}) = \bar{f}(\vec{u} \cdot \vec{u}_B) \, . \tag{16}$$

Any stationary and homogeneous solution must then be a function with symmetry around the axis of the magnetic field: $\vec{B}_{IS}$ will *isotropize* the flux in the directions orthogonal to its axis. In particular, these solutions may accommodate a dipole along $\vec{u}_B$,

$$\bar{f}(\vec{u}) = f_0 \, \left(1 - \vec{u} \cdot \vec{d} \right) \ , \tag{17}$$

with

$$\vec{d} = \frac{A^{FB}}{2\pi} \, \vec{u}_B \, . \tag{18}$$

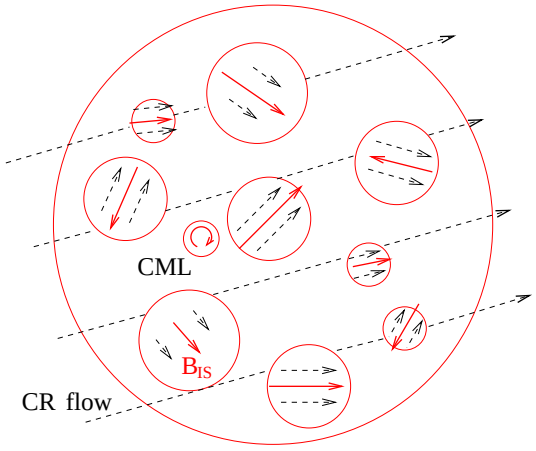

Figure 1: $\vec{B}_{IS}$ (within coherence cells of 0.1–10 pc) and cosmic ray flow. CML indicates a cosmic magnetic lens [26].

This distribution function will define (see Eq. (3)) the dipolar flux in (9) with $\vec{u}_S \to \vec{u}_B$ and $F_0 = f_0(E/c)^2$, *i.e.*, it is $\vec{B}_{IS}$ (and not the position of the sources) what fixes the direction of the CR flow in our frame, defined[1] as

$$\vec{v}_0/c = \frac{1}{N}\int \mathrm{d}\Omega\; f(\vec{u})\;\vec{u} \tag{19}$$

with $N = \int \mathrm{d}\Omega\; f(\vec{u})\,.$

The (forward or backward) direction along $\vec{B}_{IS}$ and the intensity of this dipole anisotropy will depend on boundary conditions that, in turn, will reflect the average direction of the CR flow [24, 28] at larger scales.

In Fig. 1 we plot a scheme of the CR flow within different cells that contain a regular $\vec{B}_{IS}$. This field may change randomly from cell to cell, although it has an average value $\vec{B}_R$ at kpc scales [21]. Our result above has been obtained for an observer at rest within our local IS medium. The CR anisotropy in each cell (which may have a velocity relative to us) will then follow the $\vec{B}_{IS}$ magnetic lines, with a forward or backwards direction depending on the projection of the global (average) flow $\vec{d}_R$ along $\vec{B}_{IS}$. In particular, notice that $\vec{d} \approx 0$ for a $\vec{B}_{IS}$ orthogonal to $\vec{d}_R$. Notice also that we are neglecting the velocity $v \approx 23$ km/s [29] of the Sun relative to our cell of local IS medium and the velocity $v' \approx 30$ km/s of the Earth around the Sun. These movements imply Compton-Getting [30] irregularities –in the sense that they are caused by the velocity of the observer– of order $v/c = O(10^{-4})$, introducing 10% corrections to the dominant anisotropy along $\vec{B}_{IS}$.

[1]Notice that an observer moving at $\vec{v}_0$ will see no net flux and complete isotropy. This velocity may coincide or not (for example, due to an asymmetry in the location of CR sources) with the velocity of the local plasma wind.

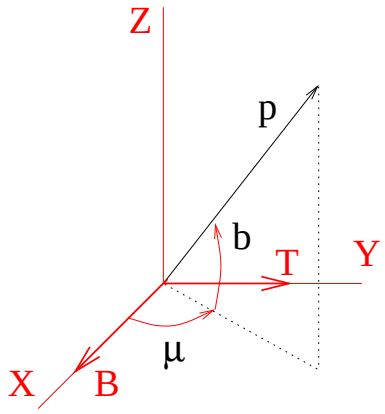

Figure 2: Coordinate system.

An important question would then be what to expect for the average CR flow. Is it $\vec{d}_R = \langle \vec{d} \rangle$ a dipole along the direction of the average magnetic field $\vec{B}_R = \langle \vec{B}_{IS} \rangle$? To unswer this question we again separate the magnetic field and the distribution function into a regular plus a fluctuating component, but now we average Boltzmann equation over larger distances, which will include different (nearby) cells:

$$\begin{aligned} f &\rightarrow f_R + \delta f \,, \\ \vec{B} &\rightarrow \vec{B}_R + \delta\vec{B} \,. \end{aligned} \tag{20}$$

Although $\delta\vec{B}$ and δf vary randomly from one cell to another, there may be correlations between both turbulent components (i.e., their relative value in each cell is not random). We will assume

$$\begin{aligned} \langle\, e\, (\vec{u} \times \delta\vec{B}) \cdot \nabla_u\, \delta f \,\rangle &= e\, \vec{u} \cdot \langle\, \delta\vec{B} \times \nabla_u\, \delta f \rangle \\ &= e\, \vec{u} \cdot \vec{T} \,. \end{aligned} \tag{21}$$

Boltzmann equation for the regular components is then

$$\vec{u} \cdot \left(\vec{B_R} \times \nabla_u\, f_R \right) + \vec{u} \cdot \vec{T} = 0 \,. \tag{22}$$

We can find consistent solutions when the correlation $\vec{T}$ is constant and orthogonal to $\vec{B}_R$. We place the axes (see Fig. 2) so that $\vec{B}_R$ and $\vec{T}$ go along the X and the Y axis, respectively, and we use the latitude b and the longitude μ to label the direction $\vec{u}$ of a CR. Taking $f_R(\vec{u}) = f_R(b, \mu)$ and

$$\nabla_u\, f_R = \frac{\partial f_R}{\partial b}\, \vec{u}_b + \frac{1}{\cos b}\, \frac{\partial f_R}{\partial \mu}\, \vec{u}_\mu \tag{23}$$

with

$$\vec{u}_b = -\sin b\, \cos\mu\, \vec{u}_\phi - \sin b\, \sin\mu\, \vec{u}_r + \cos b\, \vec{u}_z \;; \quad \vec{u}_\mu = -\sin\mu\, \vec{u}_\phi + \cos\mu\, \vec{u}_r \,, \tag{24}$$

Boltzmann equation becomes

$$-\sin\mu\,\frac{\partial f_R}{\partial b}+\tan b\,\cos\mu\,\frac{\partial f_R}{\partial \mu}+\frac{T}{B_R}\,\cos b\,\sin\mu=0\;. \tag{25}$$

This equation can be solved analytically:

$$f_R(b,\mu)=f_0\left(1+\frac{T}{f_0 B_R}\,\sin b\right)+\tilde{f}(\cos b\,\cos\mu)\;, \tag{26}$$

with f_0 a constant and $\tilde{f}$ an arbitrary function of $\cos b\,\cos\mu$. We see that the first term is just a dipole orthogonal to the plane defined by $\vec{B}_R$ and $\vec{T}$, whereas the second term may include a dipole along $\vec{B}_R$:

$$f_R(b,\mu)=f_0\,(1+t\,\sin b+s\,\cos b\,\cos\mu)\;, \tag{27}$$

with $t=T/(f_0 B_R)$ and s a constant depending on boundary conditions. The CR flux that corresponds to this distribution function (see Eq. (3)) would be

$$F_R(\vec{u})=F_0\,\left(1+\left(\vec{d}_t+\vec{d}_s\right)\cdot\vec{u}\right)\;, \tag{28}$$

where $F_0=f_0(E/c)^2$, $\vec{d}_t=-t\,\vec{u}_B\times\vec{u}_T$ and $\vec{d}_s=-s\,\vec{u}_B$. Eq. (28) expresses a key result: the global CR flow $\vec{d}_R$ does not necessarily flow along the average magnetic field $\vec{B}_R$. There may appear a second dipole anisotropy orthogonal to $\vec{B}_R$ that, added to the first dipole, could favor any direction: $\vec{d}_R=\vec{d}_t+\vec{d}_s$. Moreover, the turbulent correlation $\vec{T}$ defining this second dipole may evolve with the energy and vary its direction, which would translate into a change in the global CR flow and then in the boundary conditions that determine the dipole anistropy along $\vec{B}_{IS}$ described above.

We would like to make some final observations concerning the evolution of the anisotropy with the energy. For a standard Kolmogorov spectrum of magnetic turbulences $\lambda_\parallel$ grows with the energy like $\approx E^{0.6}$ [31], whereas $\lambda_\perp\approx r_L$ increases linearly with the CR energy. When the parallel and the transverse mean free paths become similar the propagation becomes isotropic and we should see the global CR flow (see Fig. 2). This flow, in turn, should reflect the velocity of our local IS plasma and the position and the intensity of the average CR source. Moreover, the isotropic propagation would also be a sign that r_L has reached a size similar to the region of coherence of $\vec{B}_{IS}$, since the fluctuations δB of wave number $k\approx 1/r_L$ should be $\delta B\approx B_{IS}$.

3 Small and medium scale anisotropies

A small scale anisotropy in the CR flux must be generated closer to the Earth [32, 25], at distances where the diffusive regime has not been fully established yet. It is then necessary

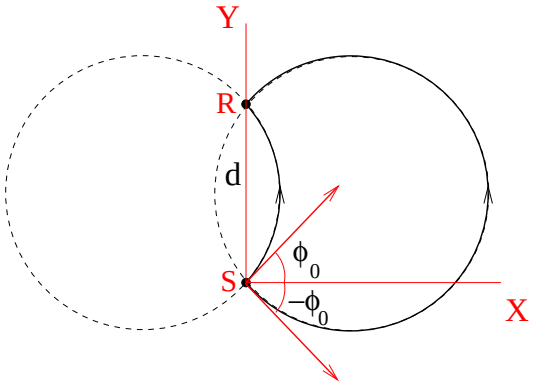

Figure 3: Trajectories between $S = (0, 0, 0)$ and $R = (0, d_\perp, 0)$ for $\vec{B}_{IS} = (0, 0, B_{IS})$.

to study the image of a point-like CR source after crossing a constant magnetic field, without the magnetic turbulences that cause the diffusion.

A particle of charge Q and energy $E \gg mc^2$ in a constant field $\vec{B}_{IS} = B_{IS}\,\vec{k}$ will describe a helix of angular frequency $\omega = B_{IS}cQ/E$ and radius $r(\mu) = c\sqrt{1-\mu^2}/\omega$. Choosing the coordinates such that at $t = 0$ the particle is at $S = (0, 0, 0)$ the trajectory reads

$$\begin{aligned} x &= -r(\mu)\,\sin\phi_0 + r(\mu)\,\sin\left(\phi_0 + \omega\,t\right) \\ y &= r(\mu)\,\cos\phi_0 - r(\mu)\,\cos\left(\phi_0 + \omega\,t\right) \\ z &= c\,\mu\,t\,, \end{aligned} \tag{29}$$

where $\mu = v_\parallel/c$ and ϕ_0 is the inital angle of $v_\perp$ with the X axis:

$$\begin{aligned} \dot{x} &= c\,\sqrt{1-\mu^2}\,\cos\left(\phi_0 + \omega\,t\right) \\ \dot{y} &= c\,\sqrt{1-\mu^2}\,\sin\left(\phi_0 + \omega\,t\right) \\ \dot{z} &= c\,\mu\,. \end{aligned} \tag{30}$$

Let us consider all the trajectories connecting the source S with an observer R located at a transverse distance $d_\perp \leq c/\omega = r_L$ and a paralel distance $d_\parallel \geq 0$. We can always rotate the axes so that R is at $(0, d_\perp, d_\parallel)$ and use the variables (μ, ϕ_0, t) to solve $(x, y, z) = (0, d_\perp, d_\parallel)$. It turns out that there is an infinite number of such trajectories, each one characterized by an integer *winding* number $n \geq n_{\rm min}$, with

$$n_{\rm min} = \text{Integer}\left[\frac{d_\parallel}{\pi\sqrt{4r_L^2 - d_\perp^2}}\right]\,, \tag{31}$$

and a (positive or negative) ϕ_0 with $|\phi_0| \leq \pi/2$. To see this it is instructive to first consider the case with $d_\parallel = 0$ (in Fig. 3), *i.e.*, with S and R in a plane orthogonal to $\vec{B}_{IS}$. The

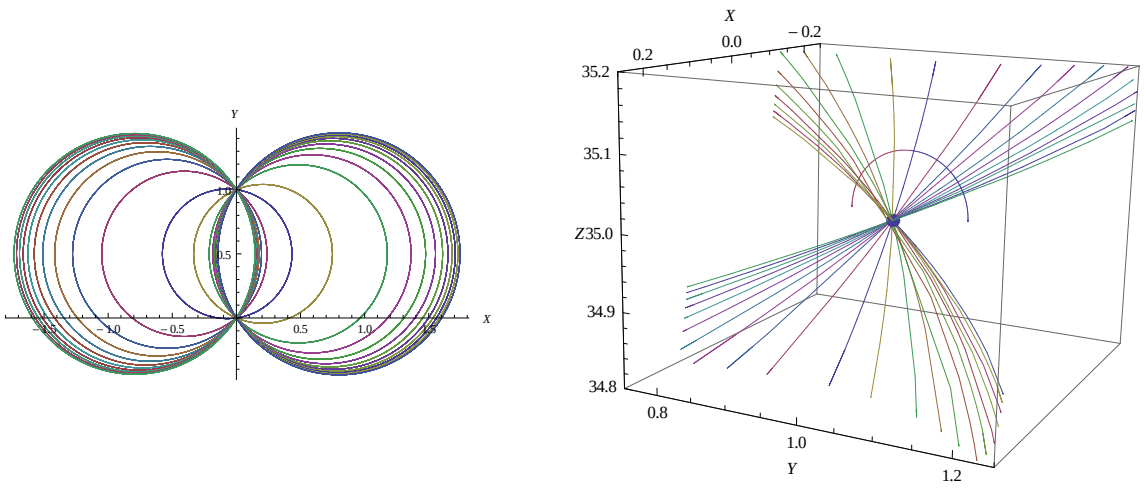

Figure 4: Twenty shortest trajectories between $S = (0, 0, 0)$ and $R = (0, 1, 35)$ for $\vec{B}_{IS} = (0, 0, B_{IS})$ and $r_L = 1$: projection on the XY plane (left) and trajectories at R (right). In the limit $d_\parallel \gg d_\perp$ the source is *seen* at R as a semi-conus of angle $\theta = \arccos d_\perp/(2r_L)$ with its axis along X and the limiting directions ($\varphi = \pm\pi/2$) defining the XY plane.

trajectories in this case have $\mu = 0$, $\phi_0^- = -\phi_0^+$ and will reach R after an arbitrary number n of turns around the left or the right circles in Fig. 3. Notice that higher values of n correspond to longer trajectories, which will provide fainter images of S (the flux scales like $1/L^2$). Adding a distance $d_\parallel$ along the $\vec{B}_{IS}$ direction the trajectories will require a non-zero value of μ to reach R, with $L = d_\parallel/\mu$ their total length. Trajectories with larger values of μ will be brighter, although this parameter is bounded by the condition $r_L\sqrt{1-\mu^2} \geq d_\perp/2$.

In Fig. 4 we plot several trajectories connecting S with R for a large ($d_\parallel = 35 r_L$) longitudinal distance. In the limit of very large $d_\parallel$ the trajectories arrive at R defining a semi-conus of directions of angle $\theta = \arccos d_\perp/(2r_L)$, with $-\pi/2 < \varphi < \pi/2$ and the limiting directions ($\varphi = \pm\pi/2$) defining the plane orthogonal to $\vec{B}_{IS}$. It is easy to see that the trajectories with direction $\varphi = 0$ and maximum μ are shorter but less dense than the ones in the extremes. As a consequence, the brightness (number of trajectories per unit length times their flux) along the semicircle scales like

$$\mathcal{B} = \mathcal{B}_0 \cos(\varphi + \pi/2) \ . \tag{32}$$

Notice also that each trajectory reaching R corresponds to a CR that left the source S at a different time, so the image at R would be the whole semicircle only for a constant and isotropic source.

Although from the previous analysis it is apparent that a nearby source could introduce small and medium scale anisotropies in the CR flux, we do not expect any sources at distances below 1 pc, which would probably introduce too large anisotropies. We find, however, another plausible mechanism for the generation of this type of anisotropies.

In [26] we have described the possible effects of a *cosmic magnetic lens*: a predominantly toroidal field configuration that may appear with a variety of sizes and magnetic strength. As deduced from Liouvilles theorem[2], an isotropic and homogeneous flux will never become anisotropic due to the action of a magnetic field. However, the large-scale dipole anisotropy discussed in the previous section could cross a nearby field configuration acting as a magnetic lens and imply point-like anisotropies of the same order. The lens would then become equivalent to a faint source of CRs but be otherwise invisible, since it does not produce nor deflect the light.

4 Comparison with the data

SuperKamiokande, TIBET, ARGO-YBF, ANTARES, MILAGRO and, more recently, HAWC have been able to distinguish from the northern sky an $O(0.1\%)$ large-scale anisotropy in the flux of 1–10 TeV CRs. IceTop and IceCube have observed with also very high statistics up to the PeV scale from the South Pole. In Table 1, we give an estimate of the results obtained in these experiments. It is remarkable that all the observations seem consistent with each other, although the higher energies seen at IceTop have not been accessible to the previous experiments nor to HAWC yet. One should notice that each experiment can access all the right ascensions (α) but only a limited region of declinations (*e.g.*, $-90^o < \delta < -25^o$ in IceCube). It becomes then difficult to estimate whether the excess and the deffect in the flux are opposite to each other ($\alpha \to \alpha \pm 180^o$, $\delta \to -\delta$) and define a dipole. Actually, in most experiments the region of maximum excess or maximum deffect is found at the limiting declinations that are accessible, suggesting that the *real* maximum is out of reach. If that is the case, the non-accessible pole will introduce a relatively less intense and broader anisotropy than the pole that can be seen by the experiment.

The data can be summarized as follows. At 1–20 TeV it reveals a dipole anisotropy that goes along $\vec{B}_{IS}$. Taking all the data from the Northern observatories and the low-energy

[2]This theorem, first applied to cosmic rays moving inside a magnetic field in [33], implies that an observer following a trajectory will always observe the same differential flux (or intensity, particles per unit area and solid angle) along the direction defined by that trajectory.

Hemisphere	Experiment	$\langle E \rangle$ [TeV]	Deficit Position		Amplitude
			R.A. [deg]	Decl. [deg]	
North	ARGO	3.6	170 to 210	-10 to 30	$3 \cdot 10^{-3}$
	MILAGRO	6	180 to 220	-10 to 0	$3 \cdot 10^{-3}$
	TIBET	6.2	170 to 210	-10 to 20	$3 \cdot 10^{-3}$
	ARGO	24	150 to 190	-10 to 30	$1 \cdot 10^{-3}$
	TIBET	300	-	-	$< 1 \cdot 10^{-3}$
South	ICECUBE	20	190 to 240	-30 to -60	$8 \cdot 10^{-4}$
	ICECUBE	400	40 to 100	-15 to -45	$7 \cdot 10^{-4}$
	ICETOP	400	70 to 110	-15 to -45	$1.6 \cdot 10^{-3}$
	ICETOP	2000	50 to 125	-25 to -55	$3 \cdot 10^{-3}$

Table 1: Summary of data on the large scale anisotropy obtained by several observatories: ARGO [34]; MILAGRO [7]; TIBET [35]; ICECUBE [36]; ICETOP [11].

IceCube results (based on the observation of atmospheric muons) we estimate

$$\ell_B = 180^o\,; \quad b_B = -60^o\,, \tag{33}$$

which is consistent with the values in Eqs. (4-5). In Fig. 5 we plot in equatorial coordinates two cones of angle 30^o with the axis along and opposite to the direction of this $\vec{B}_{IS}$. At higher energies the observations from the South Pole indicate that the anisotropy weakens, becoming of order 10^{-4}. This result is supported by TIBET (see Table 1) and, especially, by EAS-TOP [37], which at $E \approx 100$ TeV is able to *see* the movement of the Earth around the Sun (an anisotropy of amplitude 2×10^{-4}). At even higher energies (around 400 TeV) both EAS-TOP and IceCube detect an increase in the amplitude of the anisotropy and also a large change of phase, suggesting a dipole almost opposite to the initial one. Finally, at 2 PeV [11] the direction of the excess may have changed slightly towards the galactic center.

Our results in Section 2 provide a framework to interpret these observations. Above 1 TeV the effect of the heliosphere on the CR trajectories is subleading, and the dominant magnetic field is the $\vec{B}_{IS}$ in Eq. (33). The modulation above 10 TeV can then be explained if the global CR flow varies its direction with the energy. In particular, if its component along $\vec{B}_{IS}$ changes sign at ≈ 100 TeV. At these energies other effects, like the Compton-Getting of order 10^{-4} due to the velocity of the Earth, become relatively important. As the CR energy grows the possible missalignment of the anisotropy with $\vec{B}_{IS}$ would indicate that $r_L \approx R_{IS}$, where R_{IS} is the radius of coherence of the local IS magnetic field (see Fig. 2). For $B_{IS} \approx 3$ μG [16] and $E \approx 1$ PeV we obtain $R_{IS} \approx 0.3$ pc. The propagation becomes then isotropic

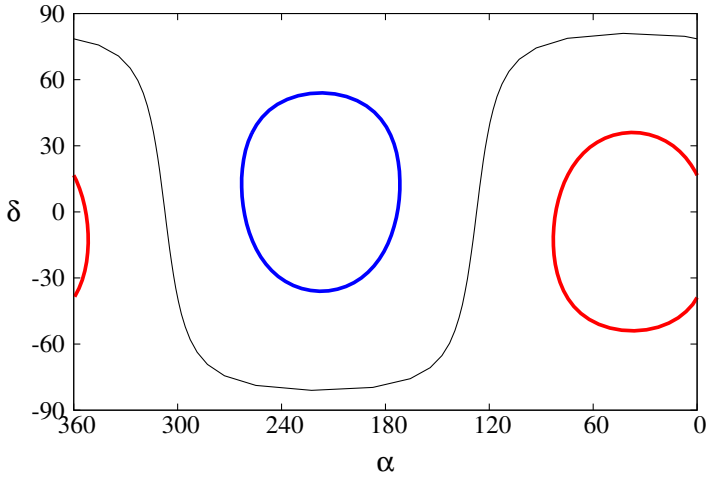

Figure 5: Dipole anisotropy along $\vec{B}_{IS}$ for $\ell_B = 180^o$ and $b_B = -60^o$ in equatorial coordinates (right ascension and declination). The thin line indicates the magnetic equator, whereas thick lines define cones of angle $\pi/4$ along the magnetic axis.

[38] and the dipole anisotropy should follow the direction of the global CR flow, which is driven by a correlation of turbulent quantities (at this scale, $\delta B = B_{IS}$ and the fluctuation δf generated by the movement of our local IS cell relative to our neighbours) and by the average magnetic field B_R. The radius $R_{IS} \approx 0.3$ pc of our local IS plasma could also be related to the appearance of the *knee* in the CR spectrum, as CRs of energy above 1 PeV could not be trapped by B_{IS} in our vicinity.

As for the low-scale anisotropies, we have described in Section 3 how the image of the dipole through a cosmic magnetic lens may introduce irregularities. These could consist of pointlike and/or longitudinal structures similar to the ones discovered by some experiments: the two regions observed by TIBET [35] and MILAGRO [40] or the four regions (which include the two former regions) found by ARGO [8]. The lens could *focus* the CR wind (see Fig. 1) and define anisotropies of order 5×10^{-4}, the amplitude that has been observed. Notice also that, since the effect of the magnetic lens on a more energetic CR will be smaller [26], the irregularities will slightly change their position and finally disappear when the energy grows. We think that region 2 in [8] –region B in [40]– could be related to the effect that we described (region 1, the most intense, seems linked to an effect of the heliotail [41]).

5 Summary and discussion

The appearence of anisotropies in the flux of charged CRs provides information about the distribution of sources and about the magnetic plasma where they have propagated on their way to the Earth. The O(10^{-3}) deficit from north galactic regions discovered by TIBET and MILAGRO seems to follow the direction of $\vec{B}_{IS}$. Using Boltzmann equation we have justified this observation and have shown that the CR flow at more global scales may modulate this anisotropy, reducing its intensity and even inverting its direction at higher energies. These features seem consistent with IceCube observations in the Southern hemisphere. We have argued that a missalignment of the dipole anisotropy with $\vec{B}_{IS}$ could be used to estimate the region of coherence of the local IS plasma. Although the appearance of anisotropies can be also understood using a diffusion equation, we think that our approach provides an alternative (and simpler) framework. In particular, Boltzmann equation averaged over different scales provides a useful picture able to describe the changes in the anisotropy with the energy.

We have also suggested a mechanism that would relate the large and the small scale anisotropies: these would appear as the image of the global dipole provided by nearby cosmic magnetic lenses (Battaner et al, 2011), that would *focus* the CR flow. Notice that the lens acts as a CR source, but that the *real* source would be the large scale-anisotropy. In particular, if this is $O(0.1\%)$, then the low-scale anisotropy will be of the same order. If the lens is seen from the Earth under a sizeable solid angle, the magnetic field B_{IS} can define linear structures like the ones described in [8].

The simplified scheme proposed here uses a number of approximations: all cosmic rays are protons (heavier nuclei of the same energy would have smaller r_L), all cosmic rays in the same data set have equal energy, or the effect of the heliosphere [41] is negligible. We think, however, that it provides an acceptable qualitative description of the data. In the near future HAWC observations from the northern hemisphere could confirm that the TIBET/MILAGRO dipole is modulated and changes sign at energies above 100 TeV.

Acknowledgments

This work has been supported by MICINN of Spain (AYA2011-24728, FPA2010-16802, FPA2013-47836, Consolider-Ingenio **Multidark** CSD2009-00064, **EPI** CSD2010-00064), and by Junta de Andalucía (FQM101, FQM108, FQM3048).

References

[1] H. Reeves, W. A. Fowler and F. Hoyle, Nature **226** (1970) 727.

[2] A. Shalchi, *Nonliner Cosmic Ray Diffusion Theories*, Springer-Verlag, 2009.

[3] F.C. Jones, Astrophys. J. **361** (1990) 162.

[4] E. Battaner, J. Castellano and M. Masip, Astrophys. J. **703** (2009) L90 [arXiv:0907.2889].

[5] M. Ahlers, Phys. Rev. Lett. **112** (2014) 021101 [arXiv:1310.5712].

[6] M. Amenomori *et al.* [Tibet AS Gamma Collaboration], Astrophys. J. **626** (2005) L29 [astro-ph/0505114].

[7] A. A. Abdo, B. T. Allen, T. Aune, D. Berley, S. Casanova, C. Chen, B. L. Dingus and R. W. Ellsworth *et al.*, Astrophys. J. **698** (2009) 2121 [arXiv:0806.2293]

[8] B. Bartoli *et al.* [ARGO-YBJ Collaboration], Phys. Rev. D **88** (2013) 8, 082001 [arXiv:1309.6182].

[9] G. Guillian *et al.* [Super-Kamiokande Collaboration], Phys. Rev. D **75** (2007) 062003 [astro-ph/0508468].

[10] S. Mangano [ANTARES Collaboration], "Skymap for atmospheric muons at TeV energies measured in deep-sea neutrino telescope ANTARES," Proceedings of the 31st ICRC, Lodz, 2009 [arXiv:0908.0858].

[11] M. G. Aartsen *et al.* [IceCube Collaboration], Astrophys. J. **765** (2013) 55 [arXiv:1210.5278].

[12] M. Santander [IceCube Collaboration], Nucl. Instrum. Meth. A **725** (2013) 85.

[13] A. U. Abeysekara *et al.* [HAWC Collaboration], "The HAWC Gamma-Ray Observatory: Observations of Cosmic Rays," in *33rd International Cosmic Ray Conference*, Rio de Janeiro, 2013 [arXiv:1310.0072].

[14] M. Y. .Zotov and G. V. Kulikov, Astron. Lett. **38** (2012) 731 [arXiv:1203.2472].

[15] R. Iuppa, Frascati Phys. Ser. **55** (2012) 61 [arXiv:1302.7184].

[16] N.A. Schwadron *et al.*, Science **343** (2014) 988.

[17] R. Ratkiewicz and L. Ben-Jaffel, and J. Grygorczuk "What do we know about the orientation of the local interstellar magnetic field?," Astron.Soc. Pac. Conf. Ser., 385, 189 194.

[18] P. C. Frisch, B-GAndersson, A. Berdyugin, V. Piirola, R. DeMajistre, H. O. Funsten, A. M. Magalhaes and D. B. Seriacopi *et al.*, Astrophys. J. **760** (2012) 106 [arXiv:1206.1273].

[19] R. Beck in *Cosmic Magnetic Fields*, Springer Verlag, Heidelberg, 2005. Edited by R. Wielebinski and R. Beck.

[20] R. Wielebinski in *Cosmic Magnetic Fields*, Springer Verlag, Heidelberg, 2005. Edited by R. Wielebinski and R. Beck.

[21] J. L. Han, "Magnetic structure of our Galaxy: A review of observations," Proceedings of the IAU, Vol. 4, S259, p455 (2009) [arXiv:0901.1165].

[22] E. Battaner in *Lecture notes and essays in Astrophysics III*, Tórculo, La Coruña, 2009. Edited by A. Ulla and M. Manteiga.

[23] B. Ruiz-Granados, J. A. Rubino-Martin and E. Battaner, Astronomy and Astrophysics **522** (2010) A73 [arXiv:1006.5573].

[24] P. L. Biermann, J. K. Becker, E. -S. Seo and M. Mandelartz, Astrophys. J. **768** (2013) 124 [arXiv:1206.0828].

[25] G. Giacinti and G. Sigl, Phys. Rev. Lett. **109** (2012) 071101 [arXiv:1111.2536].

[26] E. Battaner, J. Castellano and M. Masip, Astron. Astrophys. **527** (2011) 5 [arXiv:1006.2346].

[27] M. Pohl and D. Eichler, Astrophys. J. **766** (2013) 4 [arXiv:1208.5338]

[28] X. -B. Qu, Y. Zhang, L. Xue, C. Liu and H. -B. Hu, Astrophys. J. **750** (2012) L17 [arXiv:1101.5273].

[29] D. J. McComas, D. Alexashov, G. Bzowski *et al.*, Science. Vol. **336** (2012) 1221054.

[30] A.H. Compton and I.A. Getting, Phys. Rev. **47** (1935) 817.

[31] S. P. Swordy, Space Science Reviews 99 (2001) 85.

[32] M. Salvati, Astron. Astrophys. **513** (2010) A28 [arXiv:1001.4947].

[33] G. Lematre and M. Vallarta, Phys. Rev. 43 (1933) 89.

[34] G. Di Sciascio *et al.* (2012) [ARGO-YBJ Collaboration], J. Phys. Conf. Ser. **375** 052008 [arXiv:1112.0666 [astro-ph.HE]].

[35] M. Amenomori *et al.* (2006) [Tibet AS-gamma Collaboration], Science **314** 439 [astro-ph/0610671].

[36] R. Abbasi *et al.* (2012) [IceCube Collaboration], Astrophys. J. **746** 33 [arXiv:1109.1017 [hep-ex]].

[37] M. Aglietta *et al.* (2009) [EAS-TOP Collaboration], Astrophys. J. **692** L130 [arXiv:0901.2740 [astro-ph.HE]].

[38] F. Casse, M. Lemoine and G. Pelletier, Phys. Rev. D **65** (2002) 023002 [arXiv:astro-ph/0109223].

[39] P. Blasi and E. Amato, JCAP **1201** (2012) 011 [arXiv:1105.4529].

[40] A. A. Abdo, *et al.* (2008), Phys. Rev. Lett. **101** 221101 [arXiv:0801.3827 [astro-ph]].

[41] A. Lazarian and P. Desiati, Astrophys. J. **722** (2010) 188 [arXiv:1008.1981].